REVIEW ARTICLE

RSP Science Hub

International Research Journal on Advanced Science Hub
2582-4376
Vol. 04, Issue 12 December
www.rspsciencehub.com

Check for updates

http://dx.doi.org/10.47392/irjash.2022.074

Elastic properties of ferrite nanomaterials: A compilation and a review

Aniket Manash[1], Ratan Kumar[2], Rakesh Kumar[2], S C Pandey[2], Saurabh Kumar[2]

[1]Aryabhatta Center for Nanoscience and Nanotechnology, Aryabhatta Knowledge University, Patna, Bihar, India

[2]Vidya Vihar Institute of Technology, Bihar, Maranga, Purnea, India

Email: aniketvvit@gmail.com

Article History

Received: 12 November 2022
Accepted: 24 December 2022

Keywords:

Elastic moduli;
Poisson's ratio;
Force constant;
Bulk modulus;
Young's modulus;
Modulus of rigidity

Abstract

The Poisson's ratio, bulk modulus, Young's modulus and modulus of rigidity are the elastic moduli that are frequently employed in engineering practice. In the industrial world, elastic data are utilised to assess material strength. When considering the polycrystalline material (such as spinel ferrites, superconductors, perovskites and garnets) expose to mechanical stresses, information of the material's magnetic, electric, elastic and dielectric properties aid in finding the material's suitability for a given application. From the perspective of fundamental research, understanding elastic moduli clarifies the nature of forces (i.e interatomic and interionic) in the nanomaterial. Studies on a material's elasticity play a significant role because they are crucial for determining the strength of its binding force. The computation of elastic moduli plays a very important role in overcoming physical stresses especially in material fabrication and its industrial use. The present review focuses on the determination of elastic modulli using X-ray diffractometry and infrared spectroscopy.

1. Introduction

The most crucial aspect in assessing a material's possible applications is frequently its mechanical qualities (Ho et al.). Applications for materials as seemingly disparate as music generation from piano strings to the strength of dental porcelain to the protection of a bullet-proof vest are necessary for stiffness, tensile strength, and elastic characteristics (White). Although some high-temperature superconductors have excellent electrical and magnetic properties, their applicability is constrained by their mechanical characteristics (Hull and Murakami). The present review focuses on elastic modulus of nanoferrite material.

Large stresses form in any polycrystalline oxide material when exposed to high electric field and magnetic field, pressure and temperature (Jin, Li, and Zhang). Fracture toughness, mechanical strength, and thermal shock resistance are all represented by elastic moduli values (Aksel). Therefore, the inclusion of the material into a functional device depends greatly on its mechanical properties (Meixner and Cutler). In comparison to compositions with coarser grains, nanocrystalline ferrites are reported to have higher elastic moduli values (Pathak et al.). The average particle diameter or grain size affects the mechanical characteristics of a polycrystalline powder. Adjacent grains often have different crystallographic axes and, of course, share a grain boundary, which prevents strain motion. A material with finer grains is tougher and more durable than one with larger grains. The former can impede dislocation motion better because it has a larger total grain boundary area. It should be mentioned that reduction in grain size enhances the material's toughness in addition to

its strength. The right preparative factors can control grain size (Pathak et al.).

2. Material and Characterization methods

2.1. Synthesis of MgFe2O4 nanomaterial

Citric acid was used in the sol-gel method for $MgFe_2O_4$ synthesis. Magnesium and Iron (III) nitrate were added to DI water in a 2:1 molar ratio to ensure optimum solubility. To keep the pH at "7," drops of the NH3 solution were introduced. In order to create a gel, the combined solution was agitated at 100°C. The gel was then baked to create the ferrite tree. The $MgFe_2O_4$ nanoparticles were dried and then ground into a fine powder. To remove undesired components and enhance structural and physical behaviour, the $MgFe_2O_4$ nanoparticles were annealed for two hours at 550 degrees Celsius.

2.2. Characterization

The open atmosphere D8 facilitates X-ray diffractometer was used to acquire the XRD pattern. It was scanned at 2θ angles ranging from 20° to 75° at a wavelength of λ = 1.5406 Å. Functional group, bond length and Force constant were estimated by FTIR (Perkin Elmer) information. FTIR and XRD analyses can be used to determine a material's elastic property. The characterization of XRD and IR spectroscopy has been described in other paper (Manash Manash et al.).

3. Result and Discussion

The literature review shows that there is not much work on elastic properties of ferrite system except holmium substituted nickel zinc copper ferrite (Shinde and Lohar). The method for determining the Debye temperature (θ) and elastic constants for magnesium ferrite is described in the current paper. Our prior work on structural characterization (Manash) and IR investigation (Manash et al.) is carried on in this work. Elastic moduli that are accurate to zero porosity are calculated using the values of X-ray density (ρ), pore fraction (f), lattice constant (a) by XRD analysis (Manash) & band locations (υ) through IR spectral analysis (Manash et al.).

Equation 1, 2 have been used to express the relationship between effective mass, l, force constant, k, and bond length, r (Kagdi et al.).

$$v = \frac{1}{2\pi c}\left(\frac{k}{\mu}\right)^{1/2} \tag{1}$$

$$\mu = \left(\frac{Mo \times MFe}{Mo + M_{Fe}}\right) \tag{2}$$

Where Mo and M_{Fe} are the oxygen and iron mass, and v is the vibrational frequency.

The force constant is a derivative (second) of potential energy w.r.t the site radius and other independent parameters which are kept constant. The following equations can be used to compute the reduced mass force constant (μ) of the composition by taking into account the concentration of the cations involved and atomic weight, as well as composition's molecular mass and wave number (υ) **:**

$$k = 4\pi 2c2 \cdot \upsilon 2 \cdot \mu \tag{3}$$

Where, c = 3×10^8 m/sec which is velocity of light.

FTIR and XRD investigations can be used to determine the elastic behaviour of nanostructured materials (Sonu). Using the conventional equations provided below (Kakani and Hemarajani), the force constants at tetrahedral and octahedral complexes are determined.

$$K_t = 7.62 \times M_1 \times V_1^2 \times 10^{-2} \tag{4}$$

$$K_o = 10.62 \times \frac{M_2}{2} \times V_2^2 \times 10^{-2} \tag{5}$$

Where, Ko = octahedral site force constant, Kt= tetrahedral site force constant, M1 = tetrahedral site molecular weight, M2= octahedral site molecular weight, V_1= center frequency on tetrahedral site, and V_2 = center frequency on octahedral site.

Average force constant,

$$K = \frac{K_t + K_o}{2} \tag{6}$$

Additionally, the bond length (r) and the force constant are connected as

$$K = 17/r^3 \tag{7}$$

Using Gorter's formula (W Gorter), the R_A and R_B bond lengths have been computed.

$$R_A = (u - 1/4) \times a_{th} \times \sqrt{3} - R_o \tag{8}$$

$$R_B = (5/8 - u) \times a_{th} - R_O \quad (9)$$

Where, u = oxygen parameter, a_{th} = unit cell edge and R_0 = Bond length at octahedral site

The elastic moduli are typically 36, but they can be reduced to 3 in isotropic and homogenous materials like garnet and spinel ferrite (Patange et al.). Using IR measurements and the relation, the elastic constant and Debye temperature can be determined for the spinel ferrite material. The stiffness constant (C11, C12) can be determined using the Equations 10 and 11 which are stated as (Saafan et al.)

$$C_{11} = K_{avg}/a \quad (10)$$

$$C_{12} = (\sigma \times C_{11})/(1 - \sigma) \quad (11)$$

Where, a= lattice constant , K_t = Average force constant and σ = Poisson ratio.

Poisson ratio,

$$\sigma = 0.324\ (1 - 1.043 f) \quad (12)$$

Where, f = Nanostructured material Pore fraction.

Pore Fraction,

$$f = 1 - d/\rho \quad (13)$$

The ferrite are porous in nature and hence the pore fraction for nanostructure ferrite is in the range of ≈ 0.14-0.19 (B et al.). Shirsath et.al (Shirsath) found that the Poisson's ratio (σ) increases from 0.297 to 0.316 with increase in substitution of Zn^{2+} ions. Patange et. al (Patange et al.) found the Poisson's ratio in the range of 0.276 and 0.260 which is in agreement with the theory of isotropic elasticity.

X-ray density,

$$\rho_x = (Z \times M)/(N \times a3) \quad (14)$$

Where, Z = no of formulae unit present in the unit cell, N = Avogadro's number and M = molecular weight of sample. Sonu et.al (Kumar et al.) used the following formula to determine the elastic modulus of rare earth Ce3+ substituted strontium hexaferrite using the relation given in

equation 15, 16 and 17.

Young's modulus,

$$Y = ((C11 - C12) \times (C11 + 2C12))/((C11 + C12)) \quad (15)$$

Bulk modulus,

$$B = 1/3\ (C11 + C12) \quad (16)$$

Modulus of rigidity,

$$G = Y/(2(\sigma + 1)) \quad (17)$$

Modi et. al (Modi) used the following formula to evaluated the elastic moduli of the ferrite nanomaterials using the relation given in equation 18, 22, 23.

Modulus of Rigidity,

$$G = \rho \cdot V_s^2 \quad (18)$$

Where ρ is the X- Ray density and V_s= transverse elastic wave velocity, which is given as

$$V_L = 3^{1/2} \cdot V_s \quad (19)$$

Where, V_L is elastic wave velocity (longitudinal) and is given in terms of X- Ray density as (Modi et al.)

$$V_L = (C11/\rho)^2 \quad (20)$$

The mean elastic wave velocity (V_m) can be determined by using the values of V_L and V_s using the relation given in equation 21.

$$Vm = [3((Vl3 \times Vs3)/(Vs3 + 2\,Vl3))]^{1/3} \quad (21)$$

Poisson ratio,

$$\sigma = (3B - 2G)/(6B + 2G) \quad (22)$$

Young's modulus,

$$(E) = (1 + \sigma)\ 2G \quad (23)$$

Shinde et al. (Waldron) noted that holmium substitution resulted in higher E, K, and G values. With a rise in holmium composition x, there was a correlation between the elastic moduli increase and interatomic bonds strengthening between iron & holmium ions. Wooster et. al (Shinde and Lohar) found that there is decrease in E, B, G and θ with increase in Fe^{3+} composition. In this case the interatomic bonding is getting weakened continuously with increase in Fe^{3+}. To determine the Debye temperature (θ) of the garnets, which is provided

in equation 24, Anderson's formula (Wooster) is employed:

$$\theta = h/Kb\,[3Na/4\pi Va]^{1/3}.\,Vm \tag{24}$$

where, N_A= Avogadro's number, V_A = mean atomic volume given by equation 25

$$V_A = (M/q)/\rho \tag{25}$$

Where, M = Molecular weight and q = atom numbers (i.e., 20 for YIG and 6 for $MgFe_2O_4$) in the formula unit, h = Plank's constant and k_b =Boltzmann's constant.

The nanoferrite can be synthesized by many route but in present the samples prepared are by sol-gel are found to be porous which are shown in Figure 1. The surface morphology of MgFe2O4 produced by thesol-gel technique was investigated using SEM. The measured elastic moduli are not particularly important if correction is not done to porosity zero. Because the ferrite nanomaterial under evaluation are porous, the elastic moduli using Hosselman and Fulrath's formula (Anderson) to zero porosity using the equations 26, 27, 28, and 29 (Pore fraction= 0.14-0.19).

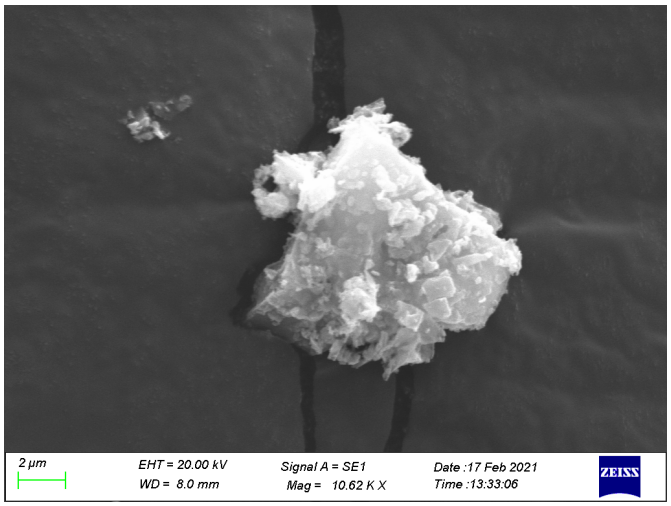

FIGURE 1. SEM imageof nanoporous Magnesium Ferrite nanomaterial annealed at 550^{o}C for 2 hours

Young's modulus corrected to zero porosity,

$$1/Eo = \{1/E[1-(3f(1-\sigma)(9+5\sigma))/(2(7-5\sigma))]\} \tag{26}$$

Modulus of Rigidity corrected to zero porosity,

$$1/Go = \{1/G[1-(15f(1-\sigma))/(7-5\sigma)]\} \tag{27}$$

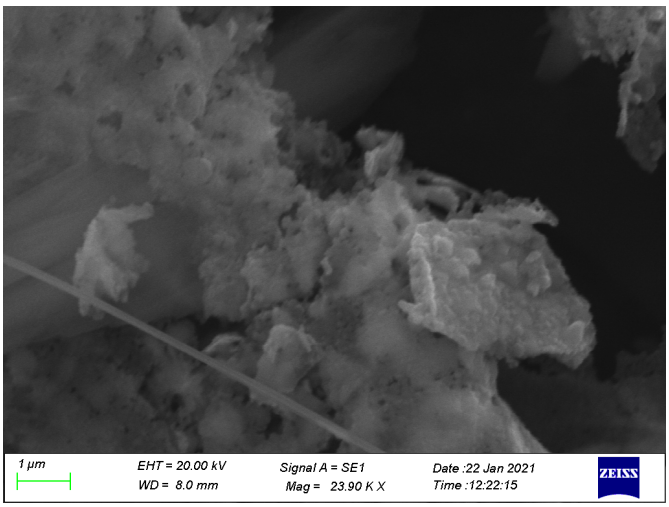

FIGURE 2. SEM image ofnanoporous Magnesium Ferrite nanomaterial annealed at 550^{o}C for 2 hours

Bulk Modulus corrected to zero porosity,

$$Bo = \rho\,[(2Vs2/(1-2\sigma)) + Vs]^2 \tag{28}$$

Poisson's Ratio corrected to zero porosity,

$$\sigma_o = E0/2G0 - 1 \tag{29}$$

The above equation shows that, Bulk Modulus corrected to zero porosity (B_0), Young's modulus corrected to zero porosity (E_0), and Modulus of Rigidity corrected to zero porosity (G_0) values exhibit regular variation comparable to corresponding elastic moduli with porosity (Modi).

4. Conclusions

Elastic moduli can be evaluated by X-ray diffraction and infrared spectral analysis and the larger value of elastic constants for nano particle compositions is due to the contraction of unit cell volume, large elastic energy and grain size reduction effect. The Poisson's ratio generally rises as dopant substitution increases. According to the isotropic elasticity theory, this value falls between the range of -1 to 0.5. With the substitution of dopants, the Debye temperature, G, E, K, C_{11} and C_{12} value increases. Rise in Debye temperature value indicates the increase in rigidity with increase in substitution of dopant in the composition. Hence, we can say that elastic moduli is the important parameter in determining strength of its binding force and plays a important function in overcoming physical stresses specially in material fabrication and industrial use.

5. Acknowledgement

The authors thank The Chairman, Mr. Ramesh Chandra Mishra, The Director, Dr. Asheshwar Yadav, The Secretary, Er. Rajesh Chandra Mishra and The Principal, Dr. Manish Kumar (Vidya Vihar Institute of Technology, Purnea - 854301, Bihar) for their encouragement and immense support to accomplish this work. It's a great pleasure to express my deep sense of unbound gratitude to Aryabhatta Center for Nanoscience and Nanotechnology, AKU, Patna, for providing infrastructure to execute this work.

References

Aksel, C. "The effect of mullite on the mechanical properties and thermal shock behaviour of alumina-mullite refractory materials". *Ceramics International* 29.2 (2003): 103–110. 10 . 1016 / S0272-8842(02)00103-7.

Anderson, O L. *Physical Acoustics*. Vol. 3. Ed. W. P.Mason. New York: Academic Press, 1965. 63–63.

B, Modi K, et al. "Elastic constants determination for Fe3+ substituted YIG through infra-red spectroscopy and heterogeneous metal mixture rule". *Journal of Materials Science* 40.5 (2005): 1247–1249.

Ho, Mei-Po P, et al. "Critical factors on manufacturing processes of natural fibre composites". *Composites Part B: Engineering* 43.8 (2012): 3549–3562. 10.1016/j.compositesb.2011.10.001.

Hull, J R and M Murakami. "Applications of bulk high-temperature Superconductors". *Proceedings of the IEEE* 92.10 (2004): 1705–1718. 10.1109/JPROC.2004.833796.

Jin, Li, Fei Li, and Shujun Zhang. "Decoding the Fingerprint of Ferroelectric Loops: Comprehension of the Material Properties and Structures". *Journal of the American Ceramic Society* 97.1 (2014): 1–27. 10.1111/jace.12773.

Kagdi, Amrin R, et al. "Influence of Mg substitution on structural, magnetic and dielectric properties of X-type barium zinc hexaferrites Ba2Zn2-xMgxFe28O46". *Journal of Alloys and Compounds* 741 (2018): 377–391. 10.1016/j.jallcom.2018.01.092.

Kakani, S L and C Hemarajani. *Text Book of Solid State Physics*. New Delhi, India: Sultan Chand & Son, 1997.

Kumar, Rakesh Kumar Singh Sonu, et al. "Structural, Elastic, and Multiferroic property of strontium ferrite nanoceramic prepared by sol-gel derived citrate precursor method". *Materials Today: Proceedings* 46 (2021). 10.1016/j.matpr.2021.03.547.

Manash, A. "Fabrication and studies of the structural, morphological and hydroelectric cell properties of K+ substituted magnesium ferrite nanomaterials prepared by a facile sol - gel route"". *J Mater Sci: Mater Electron* (2022). 10.%201007/s10854-022-08978-0.

Manash, Aniket, et al. "Studies on structural and magnetic properties of nanoporous Li+ substituted MgFe2O4 nanomaterials for its application in hydroelectric cell with other areas of science & technology". *Materials Today: Proceedings* (2022). 10.1016/j.matpr.2022.11.454.

Meixner, D L and R A Cutler. "Sintering and mechanical characteristics of lanthanum strontium manganite". *Solid State Ionics* 146.3-4 (2002): 273–284. 10 . 1016 / S0167 - 2738(01) 01027-X.

Modi, K B. "" *J. Mater. Sci* 39 (2004): 2884–2884.

Patange, S M, et al. "" *J. Appl. Phys* 109 (2011): 53909–53909.

Pathak, T K, et al. "Infrared Spectroscopy and Elastic Properties of Nanocrystalline Mg–Mn Ferrites Prepared by Co-Precipitation Technique". *Journal of Nanoscience and Nanotechnology* 8.8 (2008): 4181–4187. 10.1166/jnn.2008.AN33.

Saafan, S, et al. "" *J.Mag. Mater* 322 (2010): 2369–2374.

Shinde, Bajarang L and Kishan S Lohar. "Composition Dependent Elastic Properties of Chromium Doped NiCuZn Ferrite". *Asian Journal of Research in Chemistry* 11.2 (2018): 231–231. 10.5958/0974-4150.2018.00043.3.

Shirsath, S E. "" *Journal of Molecular Structure* 1024 (2012): 77–83.

Sonu. "Tuning of structural, elastic, luminescence, magnetic, and multiferroic properties of rare earth Ce3+ substituted strontium hexaferrite Ceramic magnetic nanomaterials for its industrial applications". *Applied Physics A* 127 (2021): 754–754. 10.1007/s00339-021-04904-z.

W Gorter, E. "" *Philips Res. Rep* 9 (1954): 295–295.

Waldron, R D. "" *Phys. Rev* 99 (1955): 1727–1727.

White, Marry Anne. *Physical Properties of Materials*. Vol. 13. Taylor and Francis: CRC Press, 2012. 978–979.

Wooster, W A. "" *Rep. Prog. Phys* 16 (1953): 62–62.

Embargo period: The article has no embargo period.

To cite this Article: Manash, Aniket, Ratan Kumar, Rakesh Kumar, S C Pandey, and Saurabh Kumar. "**Elastic properties of ferrite nanomaterials: A compilation and a review**." International Research Journal on Advanced Science Hub 04.12 December (2022): 312–317. http://dx.doi.org/10.47392/irjash.2022.074